Solvent-Dependent Structural and Electronic Behaviors of a Push−Pull Molecule: {4-[4,5-Bis(methylsulfanyl)-1,3-dithiol-2-ylidene]cyclohexa-2,5-dien-1-ylidene}malononitrile

Takaaki Hiramatsu,* Hiroyuki Yoshida, and Naoki Sato*

Institute for Chemical Research, Kyoto University, Uji, Kyoto 611-0011, Japan

Received: February 1, 2009; Revised Manuscript Received: June 18, 2009

We examined the solvent effect on the electronic absorption and infrared absorption spectra of a push−pull molecule fabricated by connecting donor and acceptor segments linked with a quinoid bridge, {4-[4,5-bis(methylsulfanyl)-1,3-dithiol-2-ylidene]cyclohexa-2,5-dien-1-ylidene}malononitrile (BMDCM), in liquid solutions. A BMDCM molecule represented by a resonance hybrid of the two canonical structures, the quinoid and benzenoid forms, showed remarkable solvatochromism. By analyzing the vibrational progressions in the electronic absorption spectra, we have grasped the behaviors of molecular structure and intramolecular charge distribution for the ground and excited states in reference to the solvent polarity.

1. Introduction

Push−pull molecules containing donor and acceptor end-groups connected by a π-conjugation bridge permit an intramolecular charge transfer (ICT), which is relevant to notable electronic properties; for example, optical nonlinearity.[1] It has been reported that the second-order nonlinear optical property of such push−pull molecules can be modified by changing the bridge.[2] These molecules are expressed by a resonance hybrid between two canonical structures for neutral and zwitterionic forms. In the report the first hyperpolarizabilities measured were analyzed for the respective molecules by considering two canonical structures in both the ground and excited states for each molecule.

We have so far been interested in push−pull molecules in terms of highly amphoteric and polar molecules, in particular, regarding controllability of the degree of ICT by choosing the bridge part connecting the donor and acceptor segments.[3,4] As a result, we designed {4-[4,5-bis(methylsulfanyl)-1,3-dithiol-2-ylidene]cyclohexa-2,5-dien-1-ylidene}malononitrile (BMDCM) whose molecular structure is shown in Scheme 1. This molecule is a push−pull molecule fabricated by connecting dithiolene-donor and dicyanomethylene-acceptor segments. We applied a quinoid as the bridge between them with suppressed ICT intended due to its cross conjugation nature.

In the previous work, we determined the ionization energy and electron affinity of BMDCM in the solid state.[5] The obtained ionization energy is smaller and the electron affinity is larger than the respective values of other molecules of a similar size, resulting in a notably small energy gap of BMDCM. These results are interpreted from the stability of both ionic and neutral states due to the resonance hybrid between the quinoid and benzenoid forms.

Since BMDCM has an intermediate structure between the two canonical structures due to the partially delocalized π-electron system at the bridge part, its electronic states should be sensitive to the molecular environments; for instance, solvent polarity in the case of the liquid solution. In studies on solvent effects on the photoabsorption energy (i.e. solvatochromism), a simple monotonic relationship is often assumed for the photoabsorption energy from the ground to excited states of the push−pull molecules versus the solvent polarity.[6,7] In such a case, the degree of ICT could be a monotonic function of the energy difference between the ground and excited states.

SCHEME 1: Resonance Hybrid for a Quinoid Form (Neutral) and a Benzenoid Form (Zwitterionic) of BMDCM[a]

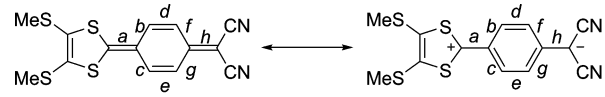

[a] Alphabet characters assign the bonds described in Section 4.2.

Würthner et al., however, demonstrated that the solvatochromism was not necessarily dependent straightforwardly on the energy difference between the ground and excited states and that further consideration was required.[8] They examined solvent effects on electrooptical absorption and electronic absorption (EA) spectra of merocyanine dyes as the push−pull molecules to determine solvent-dependent dipole moments in both the ground and excited states. As a result, they concluded that the 0−0 transition energy of the fundamental absorption feature in the EA spectrum reflected the solvent-dependent change in the degree of ICT and that its line shape changed with different solvatochromic behaviors for the respective vibronic states.

In this work, we measured EA and Fourier transform infrared absorption (FT-IR) spectra of BMDCM in various solvents and also in the gas phase. The observed EA spectra showed vibrational progressions which sensitively varied in accordance with a polarization effect in the solvation environment. We will interpret the vibrational progression observed in the EA spectra while bearing in mind the Franck−Condon principle to discuss the ICT behaviors in both the ground and excited states.

* To whom correspondence should be addressed. (T.H.) Phone: +81-75-753-4062. Fax +81-75-753-4062. E-mail: hiramatsu@kuchem.kyoto-u.ac.jp. (N.S.) Phone: +81-774-38-3080. Fax +81-774-38-3084. E-mail: naokis@e.kuicr.kyoto-u.ac.jp.

10.1021/jp9009349 CCC: $40.75
Published on Web 07/21/2009

TABLE 1: Fitting Parameters for Vibrational Progressions of Electronic Absorption Bands in BMDCM Solution Spectra Together with Relative Permittivity, Kirkwood−Onsager Function and Dipole Moment of Each Solvent and Also with Calculated c^2 As a Result

solvent	ε_r[a]	$(\varepsilon_r-1)/(2\varepsilon_r+1)$	μ/D[b]	Z_1	Z_2	$\Delta\nu_1/\mathrm{cm}^{-1}$	$\Delta\nu_2/\mathrm{cm}^{-1}$	E_{0-0}/cm^{-1}	c^2
hexane	1.8865	0.1857	0	1.582	1.688	1306	387	15 488	0.260
cyclohexane	2.0243	0.2029	0.33	1.519	1.642	1319	394	15 372	0.265
carbon tetrachloride	2.2379	0.2261	0	1.421	1.620	1321	391	15 091	0.273
benzene	2.2825	0.2305	0	1.162	1.432	1367	401	14 839	0.294
toluene	2.379	0.2395	0.375	1.205	1.446	1375	409	14 869	0.291
chloroform	4.8069	0.3587	1.04	0.956	1.293	1388	395	14 831	0.313
dichloromethane	8.93	0.4205	1.60	0.870	1.254	1390	389	14 870	0.322
1,2-dichloroethane	10.42	0.4313	1.83	0.844	1.214	1395	390	14 856	0.325
acetone	21.01	0.4651	2.88	0.761	1.288	1379	384	15 024	0.334
acetonitrile	36.64	0.4798	3.9252	0.697	1.352	1352	375	15 074	0.341

[a] Relative permittivities (at 298.0 K; 293.2 K only for dichloromethane) cited from ref 10. [b] μ is a dipole moment (1 $D = 3.354 \times 10^{-30}$ C m). Values cited from ref 11.

2. Experimental Section

BMDCM was synthesized according to the method described elsewhere.[9] Its purification was carried out with recrystallization using chloroform as the solvent followed by vacuum sublimation.

EA spectra of BMDCM in 10 kinds of solvents with different relative permittivities (Table 1)[10,11] and also in the gas phase were recorded on a Hitachi U-4000 spectrophotometer. Hexane, cyclohexane, carbon tetrachloride, benzene, and toluene were chosen as nonpolar solvents, and the other solvents were applied as polar solvents. All the solvents were carefully purified; especially chloroform, dichloromethane, 1,2-dichloroethane, and acetonitrile were dried and distilled under nitrogen atmosphere. All the solution spectra were measured at 298 K. The gas phase spectrum was measured at 537 K using in-house-made heating equipment with a quartz glass cell with a 50 mm optical path length, where the sample material was sealed.

FT-IR spectra were measured on a Nicolet Impact 400 FT-IR spectrometer to obtain structural information of BMDCM in the ground state, using a solution cell with 0.5 mm optical path length; the applied solvents were benzene, chloroform, dichloromethane, and acetonitrile to give their solutions at a concentration of 1×10^{-4} mol dm^{-3}.

Further, theoretical calculations were made using Gaussian03.[12] Molecular geometry optimization and MO calculations of BMDCM were carried out using the B3LYP functional with the 6-31G(d) basis set, enabling us to calculate fundamental vibrations. The calculated vibrational frequencies were scaled by a factor of 0.9613.[13]

3. Results

3.1. EA Spectra. Figure 1 compares EA spectra of BMDCM in various solvents and the gas phase. The molar absorption coefficient for the solution spectra is about 10^4 m^2 mol^{-1}, whereas that in the gas phase is not known because the molecular density in the gas cell could not be estimated. The spectral line shapes are significantly different between the gas-phase and the solution spectra. The gas phase spectrum shows a broad absorption band centered at 20 000 cm^{-1} without any structure. On the other hand, the solution spectra exhibit vibrational structures. The thus-observed vibrational progression indicates a large displacement in the bond lengths between the ground and excited states under the Franck−Condon principle. The energy difference among the vibrational structures is about 1350 cm^{-1}. Since this energy is close to the vibration frequency of the A-mode (Figure 2b) in the ground state as we will mention below, this vibrational mode in the excited state is likely attributed to the A-mode.

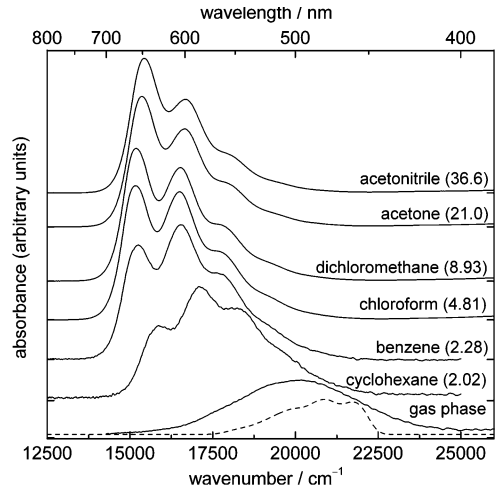

Figure 1. EA spectra of BMDCM in liquid solutions and in the gas phase. In addition to each solution spectrum, the solvent and its relative permittivity (in parentheses) are indicated. A dashed line shows the simulated spectrum. See the text for details.

The solution spectra change with the permittivity of solvents, whereas the 0−0 transition peak shows complicated behaviors. For the solvents grouped into nonpolar ones (that is, cyclohexane ($\varepsilon_r = 2.02$), benzene ($\varepsilon_r = 2.28$), and chloroform ($\varepsilon_r = 4.81$) for the time being), its shift shows bathochromic behavior, whereas for the polar solvents (that is, chloroform ($\varepsilon_r = 4.81$), dichloromethane ($\varepsilon_r = 8.93$), acetone ($\varepsilon_r = 21.0$), and acetonitrile ($\varepsilon_r = 36.6$)), it shows hypsochromic behavior. On the other hand, the intensity profile of the vibrational progression changes monotonically with increasing permittivity of the solvent; the intensity for the 0−0 transition increases with respect to that for the 0−1 transition. This behavior will be analyzed quantitatively in terms of the displacement in molecular bond lengths in the course of the electronic excitation.

3.2. Ground-State Molecular Structure in Solution. Figure 2a compares FT-IR spectra of BMDCM in four different solvents and that simulated from calculated vibrational frequencies; the observed and simulated spectra are in fairly good agreement with each other. In the wavenumber range from 1300 to 2250 cm^{-1}, four main vibrational peaks are observed. We classify these vibrational peaks by calling them A-mode, B-mode, and C-mode and providing two submodes—Ca-mode (anti-symmetric) and Cs-mode (symmetric)—in order of wavenumber from now on.

Figure 2b depicts the referred vibrational modes in the ground state that are calculated with B3LYP/6-31G(d). The frequencies of these vibrational modes are connected with the degree of

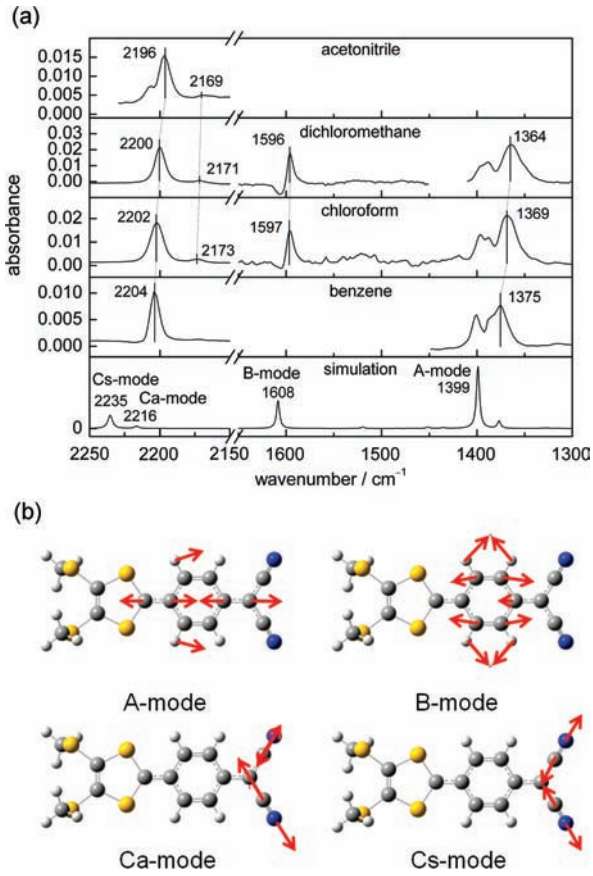

Figure 2. (a) FT-IR spectra of BMDCM in the four kinds of solvents and its simulation spectrum on the basis of the theoretical calculation using the B3LYP/6-31G(d) calculation. Observed spectra are lined up downward with decreasing permittivity of the solvent. Wavenumbers in centimeters^{-1} for notable spectral features are indicated. In the simulation spectrum, spectral assignments are shown. (b) Four vibrational modes of BMDCM in the ground state obtained with B3LYP/6-31G(d) calculation.

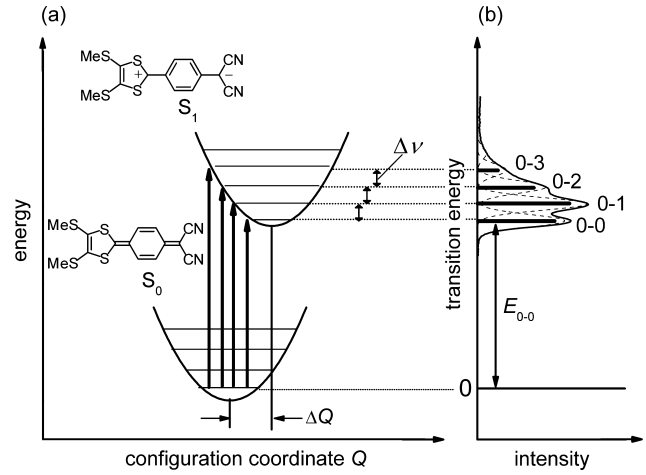

Figure 3. Schematic diagram of (a) the vibronic transition and (b) the corresponding EA spectrum. The intensity distribution of the spectral band is related to the structural difference, ΔQ, between the ground state, S_0, and the excited state, S_1. Each vibrational transition is located away from the 0−0 transition of E_{0-0} by a multiple of $\Delta\nu$.

ICT (cf. Scheme 1). The frequency of the A-mode will become high when the molecular structure is close to the quinoid form, since two related C═C bonds result in double bonds. The frequency of the B-mode will be also high for the quinoid form; however, the frequency difference between the two forms should be smaller than that in the case of the A-mode, because the difference in the bond order for C═C inside six-membered ring of the quinoid bridge is only 0.5; that is, 2 for a quinoid ring versus 1.5 for a benzene ring. The frequencies of the C≡N bonds in the C-modes will also be higher in the quinoid form, since the charge populated on the C≡N bonds can be lower than that in the benzenoid form where C≡N groups are charged more negatively.[14]

The A-mode is mainly due to the C═C stretching mode of each bond connecting the six-membered central ring and the donor or acceptor segments in BMDCM. This mode was not observed in acetonitrile solution because its frequency is close to that of the solvent. The frequency of the A-mode decreases monotonically from 1375 to 1364 cm^{-1} with increasing ε_r, indicating that the ground state structure changes from the quinoid to benzenoid forms.

The B-mode stands for C═C stretching in the six-membered ring of the quinoid bridge. Although no signal corresponding to this mode was distinguished in benzene and acetonitrile solution due to an overlap with vibrational features of the solvent, the frequency of the B-mode hardly changes in chloroform and dichloromethane solutions. The bond length connected with this mode appears to be insensitive to the solvent polarity.

The C-mode corresponds to the C≡N stretching mode for a dicyanomethylene segment. Owing to the two C≡N bonds, the vibrational peak of this mode splits into the symmetric (Cs-mode) and antisymmetric (Ca-mode) subpeaks. The symmetric stretching was observed in all the solvents, whereas the antisymmetric one was weaker than the other and was not detected in benzene. The frequency of the Cs-mode decreases from 2204 to 2196 cm^{-1} with increasing ε_r, indicating that the molecular structure in the ground state changes from the quinoid to benzenoid forms. A similar shift of the C≡N stretching frequency is reported in comparable push−pull molecules.[14]

On the basis of the observed behavior in the frequencies of these three vibrational modes, we conclude that the molecular structure of BMDCM in the ground state changes from the quinoid to benzenoid forms with the increase in the permittivity of the solvent; that is, for the change from the nonpolar to polar solvents.

4. Discussion

4.1. Analysis of the Intensity Distribution in Vibrational Progression. Figure 3 shows a schematic diagram of the vibronic transition of a BMDCM molecule with relation to the corresponding EA spectrum. The intensity profile of the vibrational progression depends on the structural difference along the configuration coordinate, ΔQ, between the ground state, S_0, and the excited state, S_1. When ΔQ denotes a displacement caused by an excitation from S_0 to S_1, it is expressed as

$$\Delta Q = \left(\sum_j \Delta r_j^2 \right)^{1/2} \tag{1}$$

where Δr_j stands for the change of the jth bond on the excitation.

The intensity distribution in the vibrational progression of an EA spectrum follows the Poisson distribution under the Franck−Condon principle. The intensity of a vibrational mode, I_m, for the transition $0-m$ is expressed as

$$I_m = I_0\left(\frac{(\tilde{\nu}_m)}{(\tilde{\nu}_0)}\right)\frac{Z^m}{m!}e^{-z} \quad (2)$$

where I_0 is a total intensity of the electronic transition, and $(\tilde{\nu})$ is the mean wavenumber of a particular transition. A fitting parameter for the Poisson distribution of the oscillator strength Z is derived from ΔQ as

$$Z = \frac{1}{2}k(\Delta Q)^2/\hbar\omega \quad (3)$$

where k and ω are the force constant and angular frequency, respectively.[15,16]

Here, we presume that k and ω are common in both electronic states and that $\tilde{\nu}_m/\tilde{\nu}_0$, k, and ω do not change over the different solvents. Under this assumption, only ΔQ is responsible for the vibrational progression as shown in Figure 3. A Z value can therefore be evaluated from an obtained EA spectrum on the basis of eq 2, which enables us to discuss the structural change of the molecule as a function of solvent polarizability.

Using eq 2, we simulated vibronic absorption spectra in the lowest energy region and fitted them to the experimental ones. We consider the lowest energy feature in the vibrational progression as owing to the 0−0 transition, characterized by the electronic excitation energy, E_{0-0}. The frequency spacing for the vibrational progression $\Delta\nu$ is taken to be the same for all the vibrational levels, assuming the harmonic oscillator. We used vibrational features from 0−0 to 0−3 for these analyses. Each vibrational level was convoluted by a Gaussian function with the full-width at half-maximum of 500 cm^{-1}. Since we noticed the simulation using only one vibrational mode cannot reproduce the observed spectral line shape in the case of solvents with small ε_r, we applied two vibrational modes characterized by $\Delta\nu_1$, Z_1, $\Delta\nu_2$, and Z_2, respectively.[17]

In this way, we evaluated the following parameters: I_0, E_{0-0}, Z_1, $\Delta\nu_1$, Z_2, and $\Delta\nu_2$. One vibrational mode with $\Delta\nu_1 \approx 1350$ cm^{-1} is assigned to the A-mode, which gives a dominant feature in the spectrum. The origin of the other mode with $\Delta\nu_2 \approx 400$ cm^{-1} is unclear and is regarded as the sum of a few different vibrational modes. Table 1 summarizes the determined parameters from the fitting together with the permittivities of the solvents.

The same analysis could, in principle, be applicable to the gas-phase spectrum. However, it shows no resolved vibrational progression so that the parameters (E_{0-0}, Z_1, $\Delta\nu_1$, Z_2, and $\Delta\nu_2$) for it were estimated by extrapolating the parameters determined for the five kinds of solution of nonpolar solvents into $\varepsilon_r = 1$. A spectrum simulated from thus-obtained parameters, shown by a dashed curve in Figure 1, reproduces the observed one fairly well, whereas the disagreement might be negligible in the low-energy region around 17 500 cm^{-1}, probably due to a hot band.

4.2. Molecular Structure and ICT. On the basis of the obtained values of Z_1, $\Delta\nu_1$, and E_{0-0}, we will examine the possible change in the molecular structure and the degree of ICT against the permittivity of the solvent, bearing in mind the resonance hybrid shown in Scheme 1. According to the resonance hybrid of the quinoid and benzenoid forms, bond lengths and the charge distribution in a BMDCM molecule change with the solvent polarity simultaneously. For example, the C═C bond length connecting with the A-mode is shorter in the quinoid form than in the benzenoid form, and the electric dipole moment is smaller in the quinoid form. To consider the solvent effects on the molecular structure and the ICT degree from now on, we introduce the Kirkwood−Onsager function (KO function), i.e. $(\varepsilon_r - 1)/(2\varepsilon_r + 1)$, since it plainly describes the enhancement of the dipole moment on a solute molecule induced by polarization due to the solvent under the approximation of continuous dielectric media.[18−20]

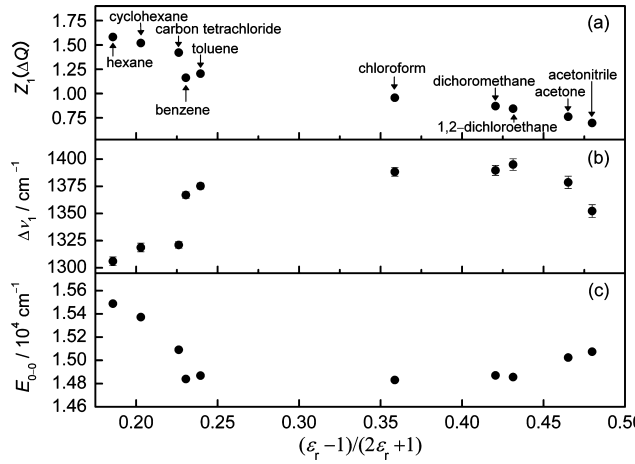

Figure 4. Fitting parameters of the electronic absorption spectra of BMDCM in the various solvents versus Kirkwood−Onsager function, $(\varepsilon_r - 1)/(2\varepsilon_r + 1)$. (a) Spectral intensity distribution parameter Z_1 for the A-mode; (b) vibrational energy interval, $\Delta\nu_1$; and (c) 0−0 transition energy, E_{0-0}.

In Figure 4, three kinds of the parameters Z_1, $\Delta\nu_1$, and E_{0-0} obtained above are plotted against the KO function. Now we focus our attention on Z_1 because it accounts for the variation of the C═C bond lengths regarding the A-mode (see Figure 2b) between the ground and electronically excited states. Figure 4a shows that Z_1 decreases almost linearly with increasing KO function, indicating that the structural difference, ΔQ, decreases with increasing KO function. In other words, the molecular structures become similar between the ground and excited states with increasing KO function or increasing polarity of the solvent.

For the analysis of electronic absorption spectra of the push−pull molecules, the valence-bond (VB) model is often applied.[21] Accepting the two canonical structures shown in Scheme 1 as valid, the ground state, S_0, and the first singlet excited state, S_1, can be described by a linear combination of the wave functions for quinoid and benzenoid canonical structures as follows:

$$\psi_{S_0} = c\psi_{\text{benzenoid}} - (1 - c^2)^{1/2}\psi_{\text{quinoid}} \quad (4)$$

$$\psi_{S_1} = (1 - c^2)^{1/2}\psi_{\text{benzenoid}} + c\psi_{\text{quinoid}} \quad (5)$$

where c is a mixing coefficient.[21]

Although our analysis of the vibrational progression above has given information on only the relative structures for the ground and electronically excited states, the VB model provides us with the resonance structure of the molecule in particular circumstances; the structures of both S_0 and S_1 states can be characterized by the single parameter, c^2. The IR results have shown that the molecular structure for S_0 is close to the quinoid form in the nonpolar solvents; for the solvents with small KO function, c^2 is nearly zero from eq 4. Equation 5 shows that the S_1 state is characterized by much contribution from the benzenoid structure at that time. With increasing KO function, c^2 will increase toward 0.5, where both S_0 and S_1 states accept

TABLE 2: Assumed Bond Lengths in a BMDCM Molecule in the Ground State and Evaluated Values of ΔQ and c^2

	bond length[a]/pm									
	a	*b*	*c*	*d*	*e*	*f*	*g*	*h*	ΔQ/pm	c^2
quinoid form[b]	137.4	145.0	144.5	134.6	134.6	144.5	145.0	137.4	19.7	0.000
gas phase structure[c]	139.0	144.1	144.1	136.1	136.1	144.0	144.0	140.1	13.2	0.166
intermediate form	142.2	141.5	141.3	136.3	136.3	141.3	141.5	142.2	0.0	0.500
benzenoid form[d]	147.0	138.0	138.0	138.0	138.0	138.0	138.0	147.0	19.7	1.000

[a] *a*−*h* stands for the bond lengths in a BMDCM molecule, as shown in Scheme 1. [b] Bond lengths in TCNQ cited from ref 22. [c] Bond lengths calculated with B3LYP/6-31G(d). [d] Bond lengths cited from ref 23.

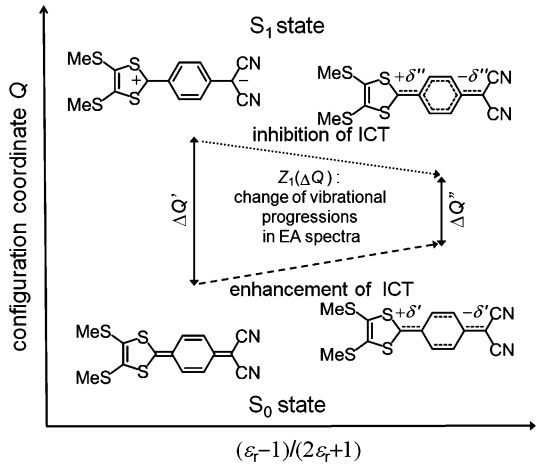

Figure 5. Schematic diagram of the relationship between the spectral intensity distribution parameter Z_1 and the degree of ICT in a BMDCM molecule for the ground and excited states, in reference to the solvent polarity (Kirkwood−Onsager function as an index). $\Delta Q' > \Delta Q''$, $0 < \delta' < \delta'' < 1$.

the intermediate structure between the quinoid and benzenoid forms. The increase of the c^2 value from zero to 0.5 leads to the increase in the degree of ICT in the S_0 state and, in contrast, the decrease in that in the S_1 state, as easily imagined from Scheme 1. These results are schematically summarized in Figure 5.

We evaluated c^2 values from Z_1 listed in Table 1 in the framework of the VB model. Since the dominant vibrational progression appearing in the EA spectra is assignable to the A-mode (Figure 2b) as mentioned in Section 3.1, ΔQ is likely expressed by the change in the bond lengths for only the bridge (from *a* to *h* in Scheme 1) upon the photoexcitation. The ΔQ values for the two canonical ($c^2 = 0$ and 1.0) and intermediate ($c^2 = 0.5$) structures can therefore be calculated from eq 1. The bond lengths in the quinoid form are taken from the crystal structure of 7,7,8,8-tetracyanoquinodimethane (TCNQ),[22] whereas those for the benzenoid form are taken from average bond lengths for various organic crystal structures.[23] ΔQ is estimated to be 19.7 pm for the S_0 state in the quinoid form and the S_1 state in the benzenoid form ($c^2 = 0$) and also for the S_0 state in the benzenoid form and the S_1 state in the quinoid form ($c^2 = 1$). In the case of $c^2 = 0.5$, the structures in the ground and excited states are identical so that $\Delta Q = 0$ pm and $Z_1 = 0$; we call this structure the intermediate form, as above. The bond lengths in the intermediate form are defined as the mean value between the quinoid and benzenoid forms.

When we assume that the bond lengths in both the ground and excited states depend linearly on the c^2 value according to eqs 4 and 5, it can be evaluated from the following relation:

$$c^2 = \frac{(19.7\ \text{pm} - \Delta Q)}{2 \times 19.7\ \text{pm}} \tag{6}$$

The MO calculation provides us with an optimized structure regarded as the molecular structure in the ground state in the gas phase, giving $\Delta Q = 13.2$ pm and $c^2 = 0.166$. The bond lengths and the values of c^2 and ΔQ for such typical cases are summarized in Table 2.

Z_1 is connected with ΔQ by eq 3. The coefficients *k* and ω in eq 3 are considered to be only weakly dependent on the solvent because its effect on them can be regarded as perturbation. In the gas phase spectrum, $Z_1 = 3.058$ is obtained by extrapolating as mentioned in Section 4.1. Using these ΔQ and Z_1 values, we evaluated $k/2\hbar\omega = 0.0176\ \text{pm}^{-2}$. Consequently, it yields the following relation:

$$Z_1 = 0.0176(\Delta Q/\text{pm})^2 \tag{7}$$

Using eqs 6 and 7, the c^2 values for BMDCM in all the solvents were calculated from Z_1 values, as summarized in Table 1. These values fall in the range from 0.26 to 0.34 and are smaller than $c^2 = 0.5$, indicating that the molecular structure in the ground state in the organic solvents is close to the quinoid rather than the benzenoid structure.

The estimation described above agrees qualitatively with the IR results shown in Section 3.2. It is known that the vibrational frequency of C−C single and C=C double bonds are around 1200 and 1650 cm^{-1}, respectively.[24] The A-mode stands for the C−C stretching of the bonds *a* and *h*, and its vibrational frequency falls in the range of 1360−1400 cm^{-1}; this suggests the bond nature is between the single and double bonds and that the molecular structure of BMDCM in the organic solvents ranges from the benzenoid to quinoid forms.

The interpretation indicated in Figure 5 will be supported by the behavior of the frequency spacing for the vibrational progression of the A-mode in the S_1 state, $\Delta\nu_1$, shown in Figure 4b. With an increase in the KO function, $\Delta\nu_1$ can be expected to increase in conjunction with the structural change from the benzenoid to quinoid forms. In practice, the observed $\Delta\nu_1$ increases from 1306 (in hexane) to 1395 cm^{-1} (in 1,2-dichloroethane), as expected, as shown in Figure 4b. However, $\Delta\nu_1$ decreases slightly with an increase in the KO factor for acetone and acetonitrile. This could be explained by the strong dipole−dipole interaction between a BMDCM molecule and the surrounding polar solvents.

A similar tendency is observed for E_{0-0}, as shown in Figure 4c. In nonpolar solvents, the observed 0−0 transition energy, E_{0-0}, exhibits simple positive solvatochromism, indicating that the dipole moment of a BMDCM molecule in the excited state is larger than that of the ground state. On the other hand, E_{0-0} demonstrates negative solvatochromism in the polar solvents. This behavior can be understood by considering the solute−solvent dipole interaction; that is, the interaction between the permanent dipole of the solute and the induced dipole of the solvent, including the contribution of the quadratic Stark effect.[25] The same kind of spectral shift is

reported on the lowest-frequency absorption band for a merocyanine dye with a zwitterionic character.[26]

These results mean that the excitation energy does not always give reliable information on the electronic state of a molecule in polar solvents, but the excitation energy is widely employed for interpreting the solvatochromism of dye solutions.[6] In contrast, our above-mentioned method based on the analysis of the vibrational progression to estimate the relative difference in molecular structure between the ground and electronically excited states appears to be applicable for a wide range of solutions of both polar and nonpolar solvents within the validity of the VB model. In addition, although this method is basically similar to that by Würthner et al.,[8] we believe our method is useful for examining the ICT characteristics because only EA spectra are, in principle, necessary for the analysis under the simple model, as in the case of the present work.

5. Conclusion

In this work, we measured EA and FT-IR spectra of a push−pull type molecule, BMDCM, in liquid solutions. Under the cognizance that the structure of this molecule is represented by the resonance hybrid between the quinoid and benzenoid forms, we analyzed the vibrational progressions in the observed EA spectra to estimate the molecular structure as well as the degree of the intramolecular charge transfer in different solvents with a wide range of permittivities. Since the quinoid bridge of a quasi-delocalized π-electron system links the donor and acceptor segments in a BMDCM molecule, the ICT degree or the molecular structure in the ground and excited states appears to be flexibly modulated by polarization effects under the solvation environment.

Acknowledgment. Computation time was provided by the SuperComputer Laboratory, Institute for Chemical Research, Kyoto University.

References and Notes

(1) Marder, S. R.; Gorman, C. B.; Meyers, F.; Perry, J. W.; Bourhill, G.; Brédas, J.-L.; Pierce, B. M. *Science* **1994**, *265*, 632.

(2) Andreu, R.; Blesa, M. J.; Carrasquer, L.; Garín, J.; Orduna, J.; Villacampa, B.; Alcalá, R.; Casado, J.; Delgado, M. C. R.; Navarrete, J. T. L.; Allain, M. *J. Am. Chem. Soc.* **2005**, *127*, 8835.

(3) Sato, N.; Kawamoto, I.; Sakuma, T.; Silinsh, E. A.; Jurgis, A. J. *Mol. Cryst. Liq. Cryst.* **1999**, *333*, 243.

(4) Sato, N.; Sakuma, T.; Yoshida, H.; Silinsh, E. A.; Jurgis, A. J. *Mol. Cryst. Liq. Cryst.* **2001**, *355*, 319.

(5) Tsutsumi, J.; Yamamoto, D.; Yoshida, H.; Sato, N. *Synth. Met.* **2008**, *158*, 934.

(6) Reichardt, C. *Angew. Chem., Int. Ed.* **1965**, *4*, 29.

(7) Reichardt, C. *Chem. Rev.* **1994**, *94*, 2319.

(8) Würthner, F.; Archetti, G.; Schmidt, R.; Kuball, H.-G. *Angew. Chem., Int. Ed.* **2008**, *47*, 4529.

(9) Hiramatsu, T.; Sasamori, T.; Yoshida, H.; Tokitoh, N.; Sato, N. *J. Mol. Struct.* **2009**, *922*, 30.

(10) Lide, D. R. Eds. *CRC Handbook of Chemistry and Physic*, 85th ed.; CRC Press: Boca Raton, 2004; pp 6−155.

(11) Lide, D. R. Eds., *CRC Handbook of Chemistry and Physic*, 85th ed.; CRC Press: Boca Raton, 2004; pp 9−45.

(12) Frisch, M. J.; Trucks, G. W.; Schlegel, H. B.; Scuseria, G. E.; Robb, M. A.; Cheeseman, J. R.; Montgomery, J.; Vreven, J. A. T.; Kudin, K. N.; Burant, J. C.; Millam, J. M.; Iyengar, S. S.; Tomasi, J.; Barone, V.; Mennucci, B.; Cossi, M.; Scalmani, G.; Rega, N.; Petersson, G. A.; Nakatsuji, H.; Hada, M.; Ehara, M.; Toyota, K.; Fukuda, R.; Hasegawa, J.; Ishida, M.; Nakajima, T.; Honda, Y. ; Kitao, O.; Nakai, H.; Klene, M.; Li, X.; Knox, J. E.; Hratchian, H. P.; Cross, J. B.; Bakken, V.; Adamo, C.; Jaramillo, J.; Gomperts, R.; Stratmann, R. E.; Yazyev, O.; Austin, A. J.; Cammi, R.; Pomelli, C.; Ochterski, J. W.; Ayala, P. Y.; Morokuma, K.; Voth, G. A.; Salvador, P.; Dannenberg, J. J.; Zakrzewski, V. G.; Dapprich, S.; Daniels, A. D.; Strain, M. C.; Farkas, O.; Malick, D. K.; Rabuck, A. D.; Raghavachari, K.; Foresman, J. B.; Ortiz, J. V.; Cui, Q.; Baboul, A. G.; Clifford, S.; Cioslowski, J.; Stefanov, B. B.; Liu, G.; Liashenko, A.; Piskorz, P.; Komaromi, I.; Martin, R. L.; Fox, D. J.; Keith, T.; Al-Laham, M. A.; Peng, C. Y.; Nanayakkara, A.; Challacombe, M.; Gill, P. M. W.; Johnson, B.; Chen, W.; Wong, M. W.; Gonzalez, C.; Pople, J. A. *Gaussian03, revision E.01*; Gaussian, Inc.: Wallingford, CT, 2004.

(13) Wong, M. W. *Chem. Phys. Lett.* **1996**, *256*, 391.

(14) Gompper, R.; Wagner, H.-U.; Kutter, E. *Chem. Ber.* **1968**, *101*, 4123.

(15) Pope, M.; Swenberg, C. E. *Electronic Processes in Organic Crystals and Polymers*, 2nd ed; Oxford University Press: New York, 1999, p 26.

(16) McCoy, E. F.; Ross, I. G. *Aust. J. Chem.* **1962**, *15*, 573.

(17) Herzberg, G. *Molecular Spectra and Molecular Structure III. Electronic Spectra and Electronic Structure of Polyatomic Molecules*; D. Van Nostrand: New York, 1966, p 142.

(18) Kirkwood, J. G. *J. Chem. Phys.* **1934**, *2*, 351.

(19) Onsager, L. *J. Am. Chem. Soc.* **1936**, *58*, 1486.

(20) Liptay, W. *Angew. Chem., Int. Ed.* **1969**, *8*, 177.

(21) Wortmann, R.; Poga, C.; Twieg, R. J.; Geletneky, C.; Moylan, C. R.; Lundquist, P. M.; DeVoe, R. G.; Cotts, P. M.; Horn, H.; Rice, J. E.; Burland, D. M. *J. Chem. Phys.* **1996**, *105*, 10637.

(22) Long, R. E.; Sparks, R. A.; Trueblood, K. N. *Acta Crystallogr.* **1965**, *18*, 932.

(23) Allen, F. H.; Kennard, O.; Watson, D. G.; Brammer, L.; Orpen, A. G.; Taylor, R. *J. Chem. Soc. Perkin Trans. II* **1987**, S1.

(24) Silverstein, R. M.; Webster, F. X. *Spectrometric Identification of Organic Compounds*, 6th ed.; Wiley: New York, 1998.

(25) McRae, E. G. *J. Phys. Chem.* **1957**, *61*, 562.

(26) Brooker, L. G. S.; Keyes, G. H.; Heseltine, D. W. *J. Am. Chem. Soc.* **1951**, *73*, 5350.

JP9009349